The Astrophysical Journal, 591:677–689, 2003 July 10

PROBING THE SIZE OF LOW-REDSHIFT Lyα ABSORBERS

Jessica L. Rosenberg
Center for Astrophysics and Space Astronomy, Department of Astrophysical and Planetary Sciences, University of Colorado, Boulder, CO 80309

Rajib Ganguly
Space Telescope Science Institute, 3700 San Martin Drive, Baltimore, MD 21218

Mark L. Giroux
Department of Physics and Astronomy, East Tennessee State University, Johnson City, TN 37614

and

John T. Stocke
Center for Astrophysics and Space Astronomy, Department of Astrophysical and Planetary Sciences, University of Colorado, Boulder, CO 80309
Received 2002 November 21; accepted 2003 March 16

ABSTRACT

The 3C 273 and RX J1230.8+0115 sight lines probe the outskirts of the Virgo Cluster at physical separations between the sight lines of 200 and 500 h_{70}^{-1} kpc. We present an analysis of available *Hubble Space Telescope* STIS echelle and *Far-Ultraviolet Spectroscopic Explorer* (*FUSE*) UV spectroscopy of RX J1230.8+0115, in which we detect five Lyα absorbers at Virgo distances. One of these absorbers is a blend of two strong metal-line absorbers at a recession velocity coincident with the highest neutral hydrogen column density absorber in the 3C 273 sight line, $\sim$350 h_{70}^{-1} kpc away. The consistency of the metal-line column density ratios in the RX J1230.8+0115 sight line allows us to determine the ionization mechanism (photoionization) for these absorbers. While the low signal-to-noise ratio of the *FUSE* spectrum limits our ability to model the neutral hydrogen column density of these absorbers precisely, we are able to constrain them to be in the range 10^{16}–10^{17} cm^{-2}. The properties of these absorbers are similar to those obtained for the nearby 3C 273 absorber studied by Tripp and collaborators. However, the inferred line-of-sight size for the 3C 273 absorber is only 70 pc, much smaller than those inferred in RX J1230.8+0115, which are 10–30 h_{70}^{-1} kpc. The small sizes of all three absorbers are at odds with the $\gtrsim$ 350 h_{70}^{-1} kpc minimum transverse size implied by an application of the standard QSO line-pair analysis. On the basis of absorber associations between these two sight lines we conclude that a large-scale structure filament produces a correlated, not contiguous, gaseous structure in this region of the Virgo Supercluster. These data may indicate that we are detecting overdensities in the large-scale structure filaments in this region. Alternatively, the presence of a galaxy 71 h_{70}^{-1} kpc from a 3C 273 absorber may indicate that we have probed outflowing, starburst-driven shells of gas associated with nearby galaxies.

Subject headings: intergalactic medium — quasars: absorption lines

1. INTRODUCTION

The structure and origin of Lyα "forest" absorbers remain uncertain despite decades of study with ground-based telescopes and more recently with the *Hubble Space Telescope* (*HST*). It has been argued that Lyα forest absorbers are related to the extended halos of bright galaxies (e.g., Lin, Börner, & Mo 2000; Lanzetta et al. 1995), that they are associated with dwarf or low surface brightness galaxies (e.g., Impey & Bothun 1997), or that they are one phase of the gaseous medium in spiral-rich galaxy groups (Morris & van den Berg 1994; Shull et al. 1998; Tripp et al. 2001; Bowen, Pettini, & Blades 2002). Alternatively, it has been proposed that they are "primordial" overdensities associated with large-scale structure, but not with any galaxy in particular (Davé et al. 1999; Stocke et al. 2001; Penton et al. 2002). It is possible that all of these scenarios are represented. Therefore, knowing the fraction of the Lyα forest associated with a given scenario, as a function of column density and redshift, is essential if we are going to use studies of the Lyα forest to understand the formation and early evolution of galaxies. The size and shape of these absorbing structures bear directly on the fraction of absorbers associated with a specific environment.

The correlation between absorbers in quasar pairs is often used to determine statistically the sizes of absorbers, particularly at high redshift (e.g., Foltz et al. 1984; Bechtold et al. 1994; Crotts et al. 1994; Dinshaw et al. 1997, 1998). These QSO sight line pair experiments yield characteristic radii for higher column density ($\log N_{\rm H\,I} \geq 14.5$ cm^{-2}) absorbers of 300–700 h_{70}^{-1} kpc, with some evidence for increasing sizes at lower redshifts (Dinshaw et al. 1998). These very large size measurements are consistent with the expectations of cosmological *N*-body simulations (Davé et al. 1999) as well as the expectations from an analytical Jeans mass theory of gravitationally bound, photoionized clouds (Schaye 2001). From a census of Lyα forest absorbers using *HST*/GHRS and STIS observations, Penton et al. (2000b, 2003) find that $\sim$40% of all local baryons reside in the forest. This estimate, however, assumes a characteristic radii for spherical absorbing structures of 100 h_{70}^{-1} kpc. It is uncertain whether this size, derived from high-redshift absorber pairs, is an appropriate measurement of the absorber's contiguous size or merely the length scale over which the absorbers are

associated with the same large-scale structure (Dinshaw et al. 1998).

Alternatively, the physical line-of-sight dimension of absorbers can be derived by assuming photoionization equilibrium, from measurements of H I column density, metal-line strengths, and the ratio of line strengths for different ionization states of the same species. The line strengths and ratios can be used to constrain metallicities and physical densities in these structures assuming photoionization equilibrium with the extragalactic ionizing flux (Bechtold 1994; Shull et al. 1999; Weymann et al. 2001; Donahue, Aldering, & Stocke 1995). The calculation of hydrogen densities from the photoionization models can then be used to infer physical sizes along the line of sight. The sizes determined for absorbers with strong, low-ionization metal lines like C II, Si II, Mg II, and Fe II (Steidel 1995; Rigby, Charlton, & Churchill 2002; Tripp et al. 2002) are much smaller than the characteristic sizes in the plane of the sky obtained from the QSO pair experiments. For example, the low-ionization absorbers with relatively weak Mg II absorption (<0.3 Å) have sizes derived from a photoionization equilibrium calculation that are less than 1 kpc (Rigby et al. 2002).

In this paper we present the case of a pair of QSOs, 3C 273 and RX J1230.8+0115, which probe the outskirts of the Virgo Cluster at physical separations between the sight lines of 200–500 h_{70}^{-1} kpc. Both sight lines contain strong ($\log N_{\rm H\,I} \sim 16$ cm^{-2}) Lyα absorption systems that have relatively low-ionization absorption-line spectra. This low-redshift pair provides us the opportunity to use both of the aforementioned size-determination methods at redshifts where we can obtain a deep galaxy census.

Tripp et al. (2002, hereafter T2002) presented an analysis of the absorption along the line of sight to 3C 273, 0°.9 away from RX J1230.8+0115 on the sky. T2002 studied the two strong absorbers at Virgo distances ($cz = 1011$ and 1586 km s^{-1}) in a STIS echelle (7 km s^{-1} resolution) spectrum of 3C 273 obtained by Heap et al. (2002). These two absorbers had been detected and studied using the Faint Object Spectrograph (FOS; Bahcall et al. 1991) and the GHRS (Morris et al. 1991; Weymann et al. 1995). More recently 3C 273 was observed with the *Far-Ultraviolet Spectroscopic Explorer* (*FUSE*; Sembach et al. 2001) allowing detections of the higher Lyman lines in both of these Virgo absorbers and O VI absorption in the 1011 km s^{-1} absorber. The 1586 km s^{-1} absorber contains only low-ionization absorption lines of C II, Si II, and Si III. Using a curve-of-growth analysis and a standard photoionization model T2002 constrained the column density ($\log N_{\rm H\,I} = 15.85$ cm^{-2}, b-value = 16.1 km s^{-1}), metallicity ([C/H] = −1.2 and [Si/C] = +0.2 in solar units), and density ($\log n_{\rm H} = -2.8$ cm^{-3}); these values determine the line-of-sight size of this absorber to be 70 pc.

We discuss the hydrogen and metal absorption lines at Virgo distances ($cz = 800$–2400 km s^{-1}) that we have identified in the available STIS echelle and *FUSE* spectra of RX J1230.8+0115 (§ 2). In § 3 we discuss in detail our inferences concerning the $N_{\rm H\,I}$, metallicity, and ionization parameter for the $cz = 1699$ km s^{-1} absorption complex based on the *HST* and *FUSE* data and the assumption of photoionization equilibrium. In § 4 we discuss the galaxy distribution around these absorbers; in § 5 we discuss the inferences based upon the coincident absorption-line pairs in these two spectra. Section 6 contains both a summary of our observational results and a discussion of the model that best fits all of the information currently available on the low-ionization, coincident velocity absorbers in these two sight lines. Throughout this paper we use $H_0 = 70$ km s^{-1} Mpc^{-1} and determine distances assuming a pure Hubble flow; the use of the Tonry et al. (2000) Virgocentric infall model reduces distances in this vicinity by ∼10% for galaxies with $cz = 1500$–1800 km s^{-1}. We cannot rule out that redshifts yield a double-valued distance solution at this local supercluster location (Tonry et al. 2000).

2. UV SPECTROSCOPY OF RX J1230.8+0115

We describe the *HST* and *FUSE* spectroscopy of RX J1230.8+0115 at recession velocities that correspond to Virgo Cluster distances, with primary emphasis on a very strong, two-component absorber at ∼1700 km s^{-1}. While the emission-line redshift of this active galactic nucleus (AGN; $z = 0.117$) allows detection of absorbers at higher redshifts than Virgo, they will not be discussed here. We first describe the Lyα and metal-line absorptions seen in an echelle mode spectrum obtained with STIS and then show the higher order Lyman series lines for the strongest two absorbers at Virgo distances obtained with *FUSE*. An analysis of a GHRS first-order grating spectrum of RX J1230.8+0115 was presented by Penton et al. (2000a), in which five of the six absorbers tabulated here were detected.

2.1. Lyα *Absorbers*

Observations of RX J1230.8+0115 were obtained with the E140M echelle mode of STIS using the 0″.2 × 0″.06 aperture on 1999 January 1 and 13 (M. Rauch, PI). The resolution of the spectrum is 7 km s^{-1} over the spectral range of 1150–1710 Å. The data reduction of the spectrum was done using the standard STIS extraction procedures. This reduction package returns heliocentric velocities that are estimated to be accurate to ±4 km s^{-1} (STIS data handbook). The RX J1230.8+0115 spectrum has a considerably lower signal-to-noise ratio (S/N) than the 3C 273 spectrum of Heap et al. (2002) because it is ∼10 times fainter. Nevertheless, the Virgo distance Lyα absorbers are strong enough to be easily detected (see also Penton et al. 2000a).

Figure 1 shows the region of Lyα absorption for Virgo velocities ($cz < 2500$ km s^{-1}) in the RX J1230.8+0115 sight line. We have binned these data by 3 pixels, giving a pixel width of 9.7 km s^{-1}, and removed a continuum that is the best by-eye fit to the damped Lyα profile. We get a best-fit value for Galactic $N_{\rm H} = 1.6 \times 10^{20}$ cm^{-2} scaled to a continuum. This fit is shown in Figure 1 (*solid line*). We also show a spline fit (*dashed line*) that was used to estimate line significance between 1218 and 1221 Å because the Galactic damped Lyα fit appears to underestimate the true continuum in this region, indicating that the AGN continuum must be rising blueward of 1221 Å. Also shown are the errors in the flux measurements. The absorption lines were fitted with Voigt profiles using VPFIT (Carswell et al. 2002).[1] We identify five lines (one of which has two components) at 4 σ or greater significance and one line at greater than 3.5 σ significance. Because there are no Galactic metal lines and no metal lines related to the associated absorbers, we identify all of the absorptions as intergalactic Lyα. Table 1 contains the following information about these absorbers:

[1] See R. F. Carswell, J. K. Webb, A. J. Cooke, & M. J. Irwin 2002 at http://www.ast.cam.ac.uk/~rfc/vpfit.html.

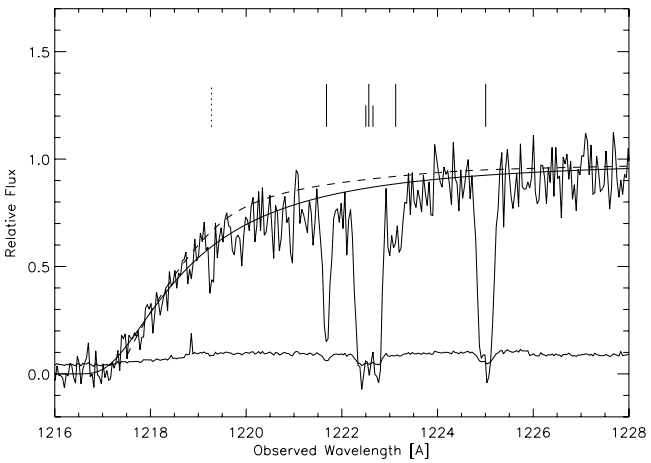

FIG. 1.—Region of Lyα absorption for Virgo velocities in the RX J1230.8+0115 sight line. The data have been binned by 3 pixels and the continuum has been fitted with a damped Lyα profile (*solid line*; see text) and a spline fit (*dashed line*). The spline fit is used to fit the region between 1218 and 1221 Å since Galactic damped Lyα fit appears to underestimate the continuum slightly in this region, indicating that the AGN continuum is rising blueward of 1221 Å. The vertical marks above the spectrum indicate the $\geq 4\,\sigma$ absorption lines detected (see Table 1). The dotted vertical mark indicates the $\geq 3\,\sigma$ absorption line that has been detected in this region. The two smaller ticks represent the positions of the metal-line components in the strong absorber blend. The lower curve shows the errors in the flux as a function of wavelength.

(1) central wavelength of the Voigt profile fit in Å, (2) central velocity of the fit (heliocentric, nonrelativistic in km s^{-1}), (3) the redshift and (4) its associated error, (5) the *b*-value and (6) its associated error in km s^{-1}, (7) the log of the H I column density and (8) its associated error in cm^{-2}—these errors include a continuum placement error derived by adding and subtracting one-third of the rms from the continuum, (9) the rest-frame equivalent width (EW) of the data (not of the Voigt profile fit) measured in mÅ, and (10) the 4 σ EW limit integrated over the same velocity width for which the EW in the ninth column was calculated (typically 3–4 times the *b*-value in the fifth column). All of these values, except for the lines at 1685 and 1721 km s^{-1}, are single-component fits determined from the Lyα absorptions alone. For these two components (1685 and 1721 km s^{-1}) we have fixed the redshifts (based upon the observed metal-line redshifts discussed in the next section) and the column densities (at $\log N_{\rm H\,I} = 16.2$ and 16.6 cm^{-2}, as discussed in § 2.4), which is why there are no quoted errors.

The 4 σ EW limits given in Table 1 indicate that all of these absorption-line detections are stronger than 4 σ except for the line at 1219.27 Å, which is 3.5 σ. Our strongest absorbers, the $z = 0.005668$ (1699 km s^{-1}) blend and the $z = 0.007680$ (2302 km s^{-1}) absorption, are both highly saturated, which makes it much more difficult to obtain accurate measurements of column densities and *b*-values. In fact, for the 1699 km s^{-1} blend, we have run an entire grid of H I column density models and found little discrimination based upon the Lyα fits alone over the range $10^{15.0}$–$10^{17.6}$ cm^{-2} (reduced χ^2 values of 1.1–2.1 over this range). Because the Lyα data are insufficient for this task, we discuss further constraints on the H I column density in the $z = 0.005668$ complex in § 2.4.

2.2. *Metal Lines Associated with the RX J1230.8+0115 Absorbers*

We have examined the RX J1230.8+0115 STIS echelle spectrum for metal lines associated with the H I absorptions discussed above and detect metal-line absorption in only the $z = 0.005668$ complex. Two component metal lines of C II, C IV, Si II, Si III, and Si IV are found associated with this complex. We used the *FUSE* data (see § 2.3) to search the region of C III absorption at this redshift, but we do not fit the C III absorption because the spectrum is noisy and the potential C III absorptions are blended with Galactic H_2. We also do not fit the Si III absorptions in the STIS echelle data because they are far down on the damping wing of Galactic Lyα and therefore in a region of very low S/N. The local continuum around the metal lines was determined with a linear least-squares fit, as the regions were determined to be flat. The metal lines were then fitted using VPFIT as for the Lyα lines. Figure 2 shows these metal lines, and the VPFIT results are summarized in Table 2. Except for the first column, which lists the identified ion, the columns have the same descriptors as Table 1. The final column gives 4 σ limits, which are also appropriate for metal-line nondetections in the other Lyα absorbers listed in Table 1. The statistical errors on the *b*-values listed in the sixth column are errors returned on the specific line profile fits in Figure 2.

In all cases where metal lines are detected, two components are detected well within the broad, saturated, Lyα profile shown at the top of Figure 2. Because the velocities of the two components are consistent between species and ionization states, we have used the velocity of the strong C II components to constrain the velocities of the 1685 and 1721 km s^{-1} components in the Lyman line analysis. The

TABLE 1
MEASUREMENTS OF VIRGO REDSHIFT Lyα ABSORBERS IN RX J1230.8+0115

λ (Å) (1)	Velocity (km s^{-1}) (2)	z (3)	Δz (4)	b (km s^{-1}) (5)	Δb (km s^{-1}) (6)	$\log N_{\rm H\,I}$ (cm^{-2}) (7)	$\Delta \log N_{\rm H\,I}$ (cm^{-2}) (8)	EW (mÅ) (9)	4 σ EW (mÅ) (10)
1219.27	889	0.002964	0.000012	17	5	13.10	0.12	46	52
1221.68	1482	0.004945	0.000004	22	2	13.68	0.04	158	56
1222.50[a]	1685	0.005621	...	23	1	16.20	...	497[b]	54
1222.65[a]	1721	0.005742	...	17	1	16.60	...	410[b]	44
1223.11	1834	0.006120	0.000023	53	11	13.47	0.09	115	56
1225.01	2302	0.007680	0.000004	33	2	14.30	0.06	360	69

[a] These values represent the best-fit model of the $z = 0.005668$ saturated blend, constrained only by the positions of the metal lines (see § 2.2).
[b] These EW values are derived from the Voigt profile fit to the line, since they cannot be separated nonparametrically in these data.

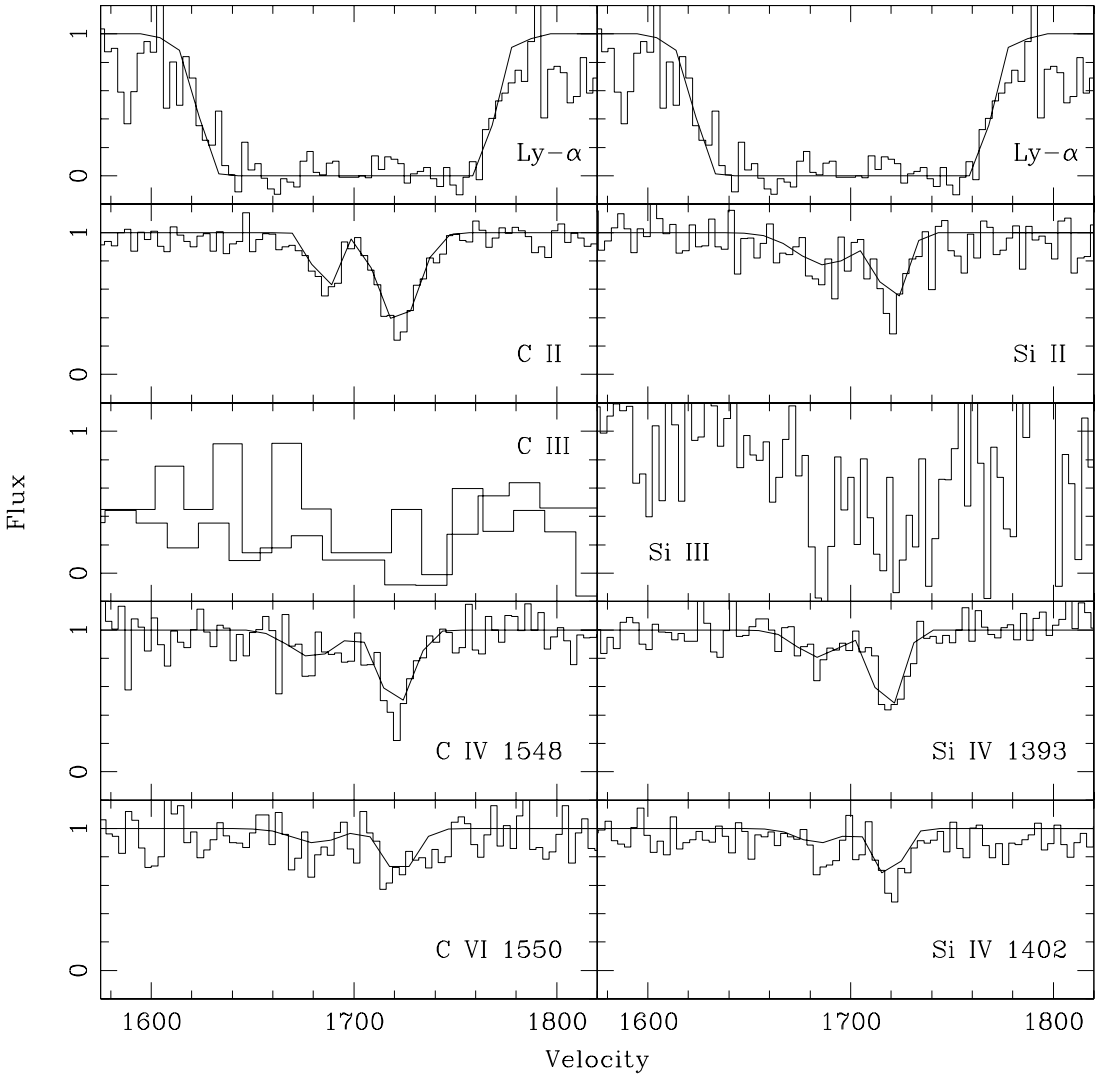

FIG. 2.—Metal lines associated with the $z = 0.005668$ absorber. We see two component lines corresponding to C II, C IV, Si II, Si III, and Si IV. The region of C III in the *FUSE* data has been shown, but it has not been fitted because it is blended with Galactic H_2. The two histograms in the C III plot show the SIC1B and SIC2A data separately. There is no fit to the Si III data because Si III is in a very low S/N region on the damping wing of Galactic Lyα, making a fit to this line highly unreliable. However, we see the same two-component absorption in the Si III and possibly C III as in the other ions. The STIS data have been displayed with no binning to show the full-resolution noise level of the spectra.

consistency of the column density ratios and the line profile shapes provides an excellent indication that the gas is photoionized and has a simple kinematic structure. A substantial contribution from collisionally ionized gas is unlikely.

The metal lines all have resolved line profiles that provide a measurement of the total *b*-value. These line widths are inconsistent with being due to pure thermal broadening since photoionization models predict temperatures below

TABLE 2
MEASUREMENTS OF METAL LINES IN THE $z = 0.005668$ ABSORBER

Ion (1)	Velocity (km s^{-1}) (2)	z (3)	Δz (4)	b (km s^{-1}) (5)	Δb (km s^{-1}) (6)	log N_{ion} (cm^{-2}) (7)	log ΔN_{ion} (cm^{-2}) (8)	EW (mÅ) (9)	4σ EW (mÅ) (10)
C II	1685	0.005621	0.000003	6	2	13.22	0.07	29	21
C II	1721	0.005742	0.000002	11	1	13.69	0.03	71	23
C IV	1679	0.005600	0.000012	15	6	12.88	0.17	24[a]	30
C IV	1720	0.005738	0.000003	10	2	13.26	0.06	66[a]	33
Si II.....	1687	0.005628	0.000014	19	7	12.42	0.14	27	26
Si II.....	1720	0.005738	0.000004	7	2	12.49	0.09	40	31
Si IV.....	1684	0.005617	0.000015	14	7	12.46	0.20	16[b]	25
Si IV.....	1718	0.005731	0.000004	8	2	12.86	0.08	43[b]	26

[a] This is the EW for the C IV 1548 line.
[b] This is the EW for the Si IV 1393 line.

20,000 K, while a thermal broadening interpretation of the line widths implies temperatures of ~90,000 K. However, the line widths of the 1720 km s^{-1} line (the S/N of the 1685 km s^{-1} line is too low to provide reliable *b*-value constraints) are consistent within 2 σ with the same amount of bulk or turbulent motion for all of the ionization states.

2.3. *FUSE Observations of Higher Order Lyman Lines*

RX J1230.8+0115 was only observed in three brief "snapshots" totaling 4031 s with *FUSE*. Nevertheless, we examined the co-added snapshots to better constrain the H I column density of the $z = 0.005668$ complex. The spectrum has a S/N of 1.1 for the SIC1B channel and 1.5 for the SIC2A channel. We have binned the data by 8 pixels for a resolution of 16 km s^{-1} per pixel. The data were processed using CALFUSE version 2.1.6.

Figure 3 shows the portion of the Lyman series detected for this absorption complex. Lyβ has not been included because it is severely blended with a Galactic O VI line, and Lyη has also been omitted because it is blended with Galactic Lyϵ. Various fits are shown spanning a plausible range in H I column density bounded by acceptable fits to the Lyα line that range from $\log N_{\rm H\,I} = 15$–17.6 cm^{-2} for the lower column density component. For all of these fits we have assumed that the two components, fixed at the metal-line velocities, have comparable metallicities and, therefore, roughly consistent relative H I column densities. The Lyman limit does not place a significant constraint on the column density because of confusion with a plethora of Galactic lines in the 915–920 Å range. Figure 3 shows that even with the *FUSE* data, it is very difficult to distinguish between these column densities. It does appear that the column density is larger than $\log N_{\rm H\,I} = 15.2$ and 15.0 cm^{-2} for the two components, and probably larger than 10^{16} cm^{-2} in both components. An assumption that the metallicity is ~6% solar as in the T2002 absorber, implies $\log N_{\rm H\,I} = 16.2$, 16.6 cm^{-2} (see § 3) and is not a bad one. However, the *FUSE* spectrum is inadequate to constrain the column densities at the high end.

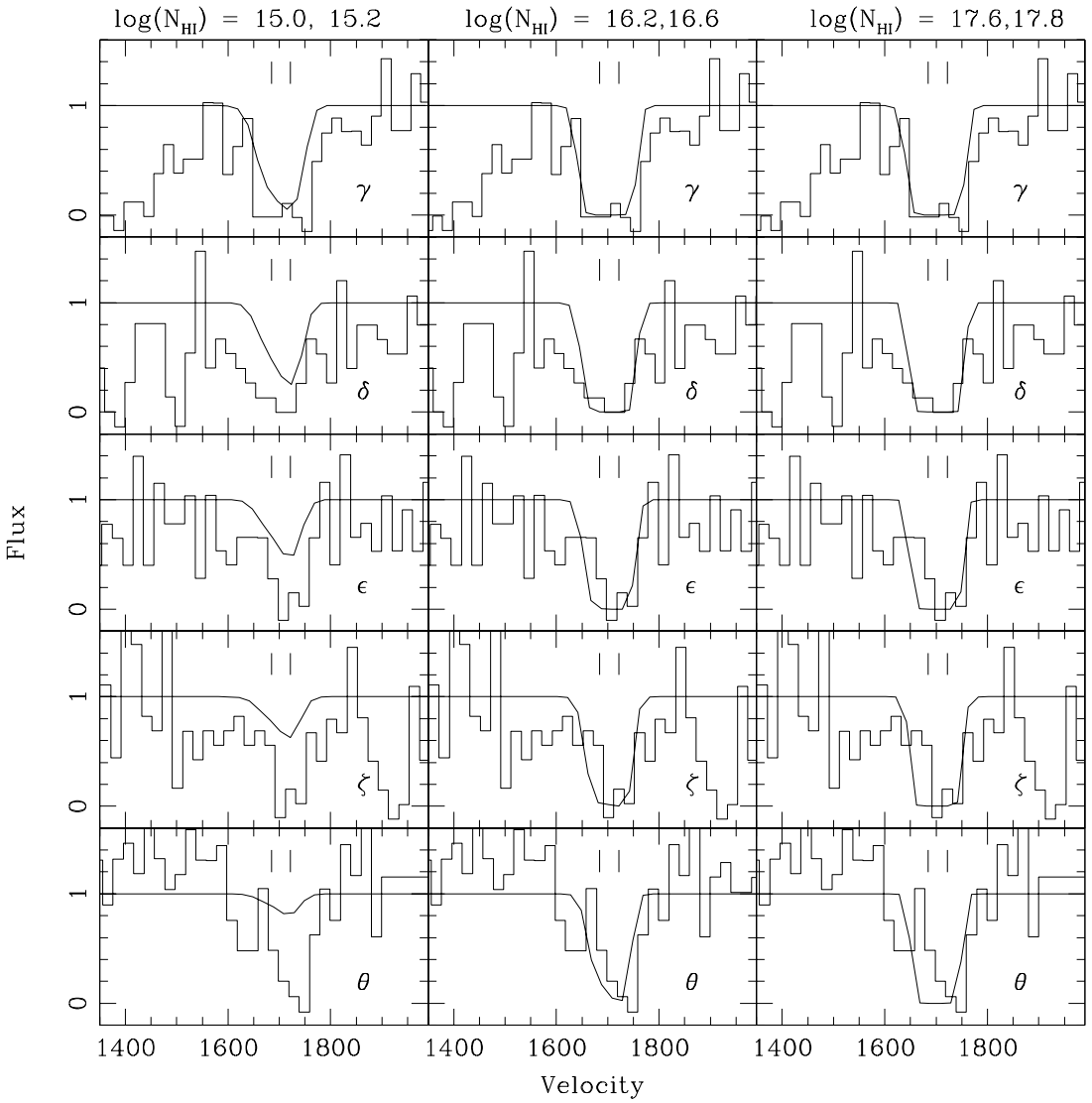

FIG. 3.—Fits to the *FUSE* data on the Lyman series lines associated with the $z = 0.005668$ absorber, spanning a plausible range of column densities based on fits to the Lyα line. The central fit is for a metallicity of 0.06 $Z_\odot$ for each component. These data indicate that fits as low as $\log N_{\rm H\,I} = 15$ cm^{-2} are excluded and that fits with $\log N_{\rm H\,I} \geq 16$ cm^{-2} are probable.

2.4. *Observational Constraints on the Column Densities of the* H I *Absorptions at* $z = 0.005668$

The saturation of the $z = 0.005668$ complex and the poor quality of the *FUSE* spectrum make it difficult to determine accurate column densities, so we list our best fits and constraints for these values, in order of the most to the least secure.

1. We place a firm lower limit on the H I column density in this line of sight by integrating the optical depth pixel by pixel within the line (Savage & Sembach 1991) using the equation

$$N_{\tau_v} = \frac{3.767 \times 10^{14}}{f\lambda_0} \sum_{i=1}^{n} \ln \left[\frac{I_c(v_i)}{I(v_i)} \right] dv_i \ , \qquad (1)$$

where $I(v_i)$ is the observed flux and $I_c(v_i)$ is the estimated continuum. If the observed flux is less than the rms in the flux, we assign the flux to be equal to the rms for that pixel; $\lambda_0 = 1215.67$ Å, the rest wavelength for the Lyα transition, and $f = 0.416$ is the oscillator strength. The lower limit to the column density from this method is 3×10^{14} cm^{-2}.

2. The consistency of the metal-line column density ratios argues for a photoionization model, while the lack of variation in the line profiles for different ions and species argues for a single phase for the gas.

3. While it is difficult to use the *FUSE* data to place accurate constraints on these two absorbers, it seems probable that the Lyϵ, Lyζ, and Lyθ absorptions require $\log N_{\rm H\,I} > 16.0$ cm^{-2}.

4. We have used the redshifts of the C II absorption lines in this complex to fix the positions of the H I components. For the Lyα saturated absorption complex, the best fit ($\chi^2_\nu = 1.1$) from VPFIT is found when $\log N_{\rm H\,I} = 15.0$ cm^{-2} for the $z = 0.00562$ component and $\log N_{\rm H\,I} = 15.2$ cm^{-2} for the $z = 0.00574$ component. But these column densities are not consistent with the strong, albeit noisy, higher Lyman series absorption seen with *FUSE*. Further, as we discuss in § 3, if the gas is photoionized such low values of $N_{\rm H\,I}$ imply metallicities of order solar to account for the C II and C IV column densities. Metallicities greater than 0.3 solar are unlikely, as this corresponds to the metallicity of the intracluster medium at the center of the Virgo Cluster as derived from the X-ray observations (Hwang et al. 1997). By comparison, the metallicity found in the 3C 273 strong absorber at this velocity is 6% solar (T2002). While we can derive acceptable Lyα line fits for all column densities tried up to $\log N_{\rm H\,I} = 17.8$ cm^{-2} for the $z = 0.00562$ component and $\log N_{\rm H\,I} = 18.0$ cm^{-2} for the $z = 0.00574$ component, for column densities exceeding 10^{17} cm^{-2} the b-values derived to fit the Lyα equivalent widths are unrealistically low (8–14 km s^{-1}) for these absorbers. While such low measured values are possible if these absorbers have no turbulent motion (Davé & Tripp 2001), the presence of C IV and Si IV at comparable strength to C II and Si II make such low values very unlikely; e.g., the 3C 273 absorber studied by T2002 has no C IV and $b = 16.1$ km s^{-1}. We conclude that the most likely column density range that fits all the data is $N_{\rm H\,I} = 10^{16}$–10^{17} cm^{-2}.

5. If we assume that the metallicities of the components are the same as for the T2002 absorber in the 3C 273 sight line, we derive column densities of 1.6×10^{16} and 4.0×10^{16} cm^{-2}. The Lyα fit has a $\chi^2_\nu = 2.04$ (probability = 0.005), insignificantly different from the nominal best fits discussed above. These are the values shown in the middle panel of Figure 3 and are clearly consistent with the *FUSE* data. These values also have reasonable, although somewhat low, b-values for low-z Lyα absorbers of 17 and 16 km s^{-1}, respectively.

In conclusion, while we cannot prove based upon the data alone that the column density of these two absorbers is $\log N_{\rm H\,I} = 16.2$ and 16.6 cm^{-2} and that the metallicities are a few percent of solar, these values are the most probable for this absorption complex. Our "best-guess" model has $\log N_{\rm H\,I} = 16.2$, 16.6 cm^{-2} derived from the assumption that $Z = 0.06\ Z_\odot$, as in the T2002 absorber, for the two components.

3. A PHOTOIONIZATION MODEL OF THE $z = 0.005668$ ABSORBER COMPLEX

Because the highly saturated Lyα absorption profile and the poor quality of the *FUSE* spectrum make it difficult to constrain the H I column density precisely, we use the metal-line ratios to determine the properties of the gas before returning to analyze the H I absorption informed by the metal-line data. As summarized in Table 2, the metal lines are associated with two velocity components, one at $v \sim 1685$ km s^{-1} and one at $v \sim 1721$ km s^{-1}. These velocity components show no differences in structure as a function of species or ionization state, suggesting that the gas is in a single phase. Several lines of argument favor a photoionization model for the gas: (1) for the $v \sim 1721$ km s^{-1} component, limits on the line width constrain the temperature of the gas to be less than 105,000 K; (2) the relative Si II and C II column densities of both components are compatible with equal ionization fractions (after accounting for the relative abundances of Si and C); and (3) purely collisional ionization is inconsistent with the Si II/C II ratio for temperatures above 20,000 K (Sutherland & Dopita 1993). However, at temperatures below 20,000 K extremely little C IV or Si IV would be observed.

Thus, we consider the properties of the gas at each velocity in turn assuming that (1) all observed ionization stages of carbon and silicon are associated with the same gas, which is compatible with the ratio of column densities, as we will show; (2) the gas is primarily photoionized, which is consistent with the predominance of lower ionization stages for carbon and silicon and with the consistency of the column density ratios; and (3) the gas is approximated as a plane-parallel slab illuminated by a quasar-dominated spectrum (Shull et al. 1999; Haardt & Madau 1996) with an intrinsic power-law spectrum of spectral energy index $\alpha = 1.8$.

To model the physical properties of the gas we have constructed a large grid of photoionization models using the photoionization code Cloudy (Ferland 1996). The calculated column densities of C II, C IV, Si II, Si III, and Si IV depend primarily on the metallicity, H I column density, and ionization parameter $U = n_\gamma/n_{\rm H}$. Relative to these parameters, the uncertainty in the spectral shape of the extragalactic background radiation contributes a negligible difference to the models.

At this point, we examine the dependence of the N(C II)/N(C IV) and N(Si II)/N(Si IV) column density ratios on the ionization parameter. For a given metallicity and H I column density, we can plot these ion ratios versus U, as shown

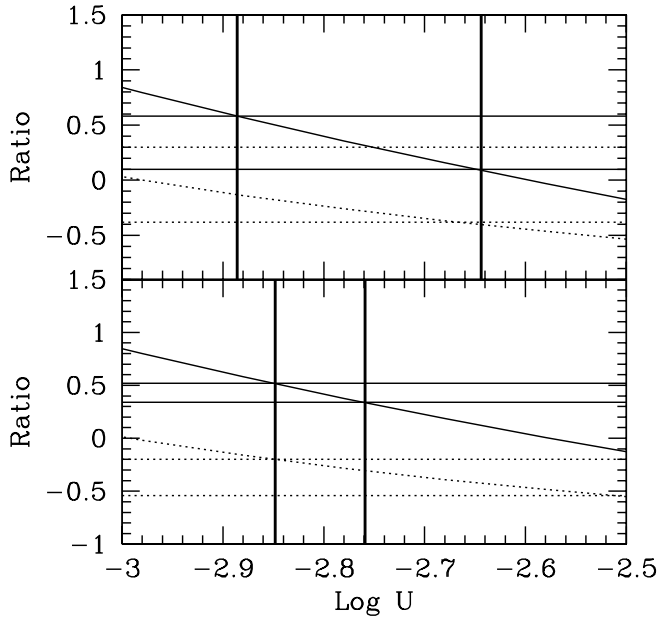

FIG. 4.—Calculated column density ratios vs. ionization parameter U for models approximating the absorber at 1685 km s^{-1} (*top*) and at 1721 km s^{-1} (*bottom*). Solid curves indicate the changing N(C II)/N(C IV) ratio, and dotted curves indicate the changing N(Si II)/N(Si IV) ratio. Solid (*dotted*) horizontal lines indicate the 1 σ uncertainty about the measured values of N(C II)/N(C IV) [N(Si II)/N(Si IV)]. The thick vertical lines indicate the range in log U consistent with the observations of the N(C II)/N(C IV) ratio. As shown, the range in log U is also consistent with the N(Si II)/N(Si IV) ratios in the 1721 km s^{-1} absorber. The range in log U in the 1685 km s^{-1} absorber is marginally inconsistent with the N(Si II)/N(Si IV) ratios. We have chosen to use the more secure N(C IV)/N(C II) measurements to set the acceptable range in the ionization parameter.

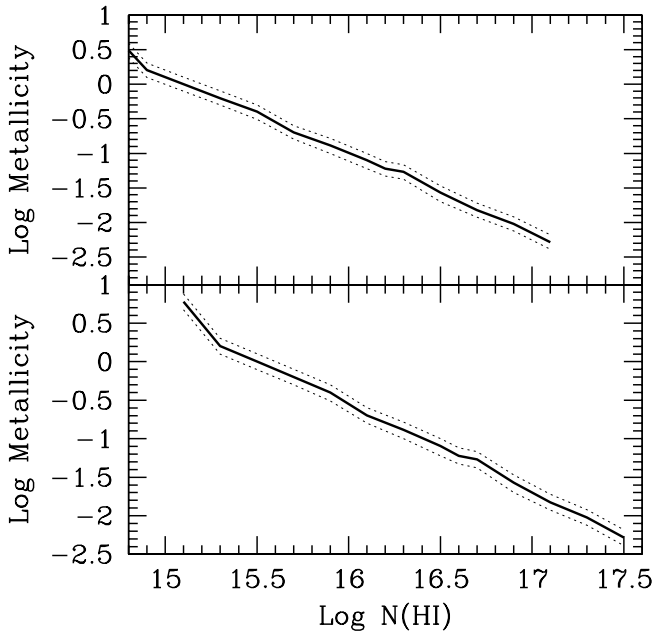

FIG. 5.—Range in metallicity consistent with observed column densities for photoionization models approximating the absorber at 1685 (*top*) and at 1721 km s^{-1} (*bottom*). The dotted curves show the model uncertainty in this relation.

in Figure 4. In this figure we assume the metallicity to be (C/H) = 0.06 solar (corresponding to $\log N_{\rm H\,I} = 16.2$ and 16.6 for the 1685 and 1721 km s^{-1} absorbers, respectively), our best-guess model based upon the constraints described in § 2.4. Finally, closest agreement with the observed column densities of N(Si II) and N(Si IV) is obtained by assuming log(Si/C) $\approx +0.1$, which is also compatible with the conclusions of T2002 for the absorber toward 3C 273. The range in ionization parameter consistent with the carbon line observations is $-2.89 < \log U < -2.65$ for the gas at $v \approx 1685$ km s^{-1} and $-2.85 < \log U < -2.76$ for the gas at $v \approx 1721$ km s^{-1}. This range is also consistent with the N(Si II)/N(Si IV) column density ratio, so our one-phase approximation likely remains a reasonable one. These ranges indicate the uncertainty in U, for a *given* metallicity or H I column density.

To explore the sensitivity of U to the H I column density and metallicity, we step through column density within the range, $\log N_{\rm H\,I} = 14.7$–17.5 cm^{-2}, corresponding to a metallicity in the range 6–0.005 $Z_\odot$ such that the absolute column density of each metal ion is always consistent with the values in Table 2. The range in U is fairly insensitive to $N_{\rm H\,I}$ and Z; the expanded range becomes $-2.9 < \log U < -2.3$ and $-2.9 < \log U < -2.4$ for the gas at $v \sim 1685$ and 1721 km s^{-1}, respectively, over this range of $\log N_{\rm H\,I}$.

For a single-phase model, as suggested by the simplicity of the metal-line profiles, the allowed range in ionization parameter may be translated into a range in density if the intensity of the extragalactic ionizing background is known. Shull et al. (1999) estimate a mean intensity of $J_\nu \sim 1\times 10^{-23}$ ergs s^{-1} cm^{-2} sr^{-1} Hz^{-1} at 1 ryd by summing the contribution from quasars, which is consistent with J_ν calculated using more direct methods such as the low-z proximity effect, truncation of H I disks, and limits on Hα from extragalactic clouds (Bechtold 1994; Shull et al. 1999; Maloney 1993; Weymann et al. 2001; Donahue et al. 1995). The implied range in hydrogen density for these absorbers is $n_{\rm H} = (1$–$5) \times 10^{-4}$ and $(1$–$3) \times 10^{-4}$ cm^{-3} for the $v \sim 1685$ and 1721 km s^{-1} components, respectively. These densities correspond to overdensities of $\delta \sim 600$–3000 and 600–1800 for the two absorbers in units of the mean baryon density at $z = 0$. These densities are an order of magnitude lower than those inferred for the gas toward 3C 273 (T2002).

The extent of the gas associated with the absorption over the possible range of $N_{\rm H\,I}$ or metallicity is 0.8–50 kpc. However, the requirement that our models reproduce the absolute C II and C IV column densities, as well as their ratios, means that the $N_{\rm H\,I}$ and metallicity for successful models are highly correlated, as shown in Figure 5. Since the line-of-sight extent of the gas in our models is derived by dividing $N_{\rm H\,I}$ by the mean hydrogen density, and since the range in mean hydrogen density compatible with line ratios varies slowly with $N_{\rm H\,I}$ there is also a good correlation of extent with assumed metallicity. Figure 6 shows the line-of-sight extent of the gas as a function of the assumed metallicity. Very large extents are possible only by invoking $Z \leq 10^{-2}$ $Z_\odot$; these low metallicities also require $\log N_{\rm H\,I} > 17$ cm^{-2}, which yield unrealistically low b-values (see § 2.4). For the probable lower limit on $\log N_{\rm H\,I} \geq 16.0$ cm^{-2} suggested by the *FUSE* detection of higher order Lyman lines, the metallicity of these structures must be $\lesssim$10%–20% solar, in agreement with their location well away from the Virgo core.

For our best-guess model, $\log N_{\rm H\,I} = 16.2$ and 16.6 cm^{-2}, derived from the assumption of $\sim$6% solar abundances (consistent with the nearby 3C 273 absorber) we find sizes along the line of sight of $\sim$10–30 kpc. The T2002 analysis of

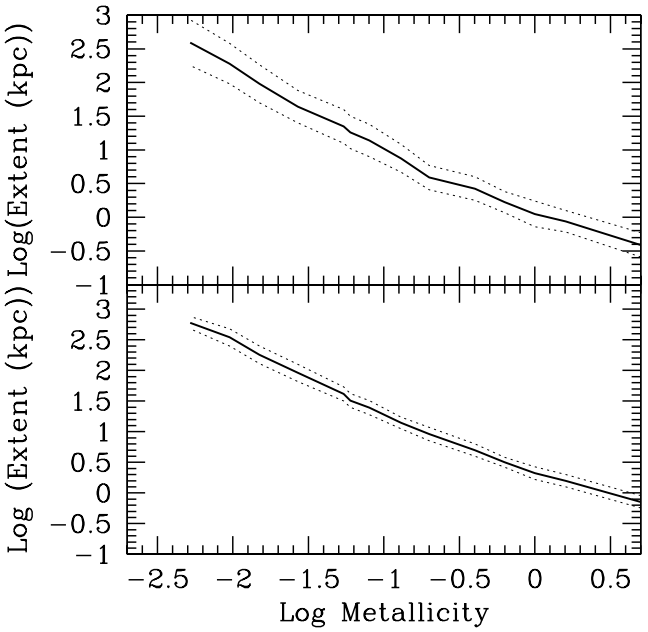

FIG. 6.—Calculated line-of-sight extent vs. metallicity parameter for models approximating the absorber at 1685 km s^{-1} (*top*) and at 1721 km s^{-1} (*bottom*). The dotted lines represent the model uncertainty in this relation.

the 3C 273 absorber at the same velocity infers an even smaller line-of-sight depth of only 70 pc. We cannot rule out that the column densities are an order of magnitude higher than our best guess, with corresponding metallicities of $\leq 0.01\ Z_{\odot}$ and much larger line-of-sight extents. However, the observations together with those analyzed in T2002 suggest that a very thin ($\sim$10 kpc) "ribbon" or "sheet" of photoionized gas with abundances of a few percent of solar extends for several hundreds of kiloparsecs through this region on the outskirts of the Virgo Cluster or that there are several thin gaseous structures lying along a large-scale filament in this region. Given the expected velocity dispersion of galaxies in the outskirts of a cluster like Virgo (100–300 km s^{-1}), it is unlikely that a single thin "ribbon" would be dynamically stable for the length of time required to form it ($\gtrsim 10^9$ yr).

4. GALAXY IDENTIFICATION IN THE VICINITY OF RX J1230.8+0115 AND 3C 273

Our knowledge of galaxies near the RX J1230.8+0115 sight line at Virgo Cluster velocities comes from four sources: (1) an augmentation to the Center for Astrophysics (CfA) redshift survey (Grogin, Geller, & Huchra 1998), (2) a pointed survey using Las Campanas Observatory (LCO) to obtain redshifts around 3C 273 (Morris et al. 1993), (3) two deep pointed surveys using multiobject spectroscopy from the Wisconsin-Indiana-Yale-NOAO (WIYN)[2] 3.5 m and Las Campanas Observatory (LCO) Du Pont 2.5 telescopes (J. T. Stocke et al. 2003, in preparation), and (4) the Sloan Digital Sky Survey (SDSS) early data release (EDR; Stoughton et al. 2002). The pointed galaxy surveys were designed to investigate the relationship between the Lyα forest absorption systems along these sight lines and the galaxies.

Grogin et al. (1998) obtained spectroscopic data to augment the CfA redshift survey in the 3C 273 region so that the survey would be virtually complete down to $m_b \leq 15.7$ ($M_B \leq -16.2$ at 24.3 Mpc for $cz = 1700$ km s^{-1}) in a region bounded by $11^{\rm h}30^{\rm m} \leq \alpha \leq 13^{\rm h}30^{\rm m}$ and $-3\overset{\circ}{.}5 \leq \delta \leq +8\overset{\circ}{.}5$. This region includes both the 3C 273 and RX J1230.8+0115 sight lines and extends several Mpc around these sight lines at Virgo distances. The SDSS EDR spectroscopic survey includes a strip around the north Galactic cap at $\delta = 0^{\circ}$ that extends up to $\delta = 1\overset{\circ}{.}3$, covering the declination of RX J1230.8+0115 but not the declination of 3C 273. The nominal completeness limit for this spectroscopic survey is $r < 17.8$, at least 2 mag fainter than the augmented CfA survey in this region.

Morris et al. (1993) also conducted a galaxy redshift survey around 3C 273 for which they claimed completeness to $m_B \sim 19$ over a region with a 60′ radius in R.A. and 40′ radius in declination from the quasar. While RX J1230.8+0115 is just beyond the southern edge of this survey region, it includes galaxies up to $\sim$700 h_{70}^{-1} kpc to the north and west of RX J1230.8+0115.

More recently, J. T. Stocke et al. (2003, in preparation) have conducted a multiobject spectroscopy survey in the region, including (1) an LCO slit-mask spectroscopy survey around RX J1230.8+ 0115, (2) an LCO slit-mask survey around 3C 273 to augment the Morris et al. (1993) observations, and (3) a WIYN/HYDRA fiber-fed spectroscopic survey in the region between 3C 273 and RX J1230.8+0115 centered at $\alpha = 12^{\rm h}30^{\rm m}$, $\delta = +1\overset{\circ}{.}67$. A preliminary discussion of the observing setups, data reduction, and analysis of the LCO and WIYN data can be found in McLin et al. (2002). A more complete discussion of the techniques and results for all sight lines observed will be presented later (J. T. Stocke et al. 2003, in preparation). We review what has been done so far in the 3C 273/ RX J1230.8+0115 region by this ongoing survey here:

1. The LCO observations surrounding RX J1230.8+0115 consist of spectra for 43 galaxies, or $\sim$78% of the galaxies down to $m_B \sim 20$ (corresponding to $M_B \leq -12$ at the distance of the $z = 0.005668$ complex) out to a radius of 5′ (36 h^{-1} kpc at this distance) from the target and 21% of the galaxies out to 15′. No galaxies were found at the redshifts of any of the Virgo Cluster absorbers, although several galaxies associated with absorbers behind Virgo were found.

2. The LCO slit mask spectroscopy around 3C 273 is 100% complete down to $m_B \sim 19.5$ out to a 10′ radius. We obtained redshifts for five galaxies that were missed by Morris et al. (1993), probably as a result of a classification error made by the automated galaxy-finding software employed (see J. T. Stocke et al. 2003, in preparation) despite their claim of 100% completeness over a large region. Seventy-seven galaxies fainter than the Morris et al. (1993) magnitude limit were also observed.

One of the five galaxies missed by Morris et al. (1993) is a relatively bright ($M_B = -14.5$) galaxy 71 h_{70}^{-1} kpc from 3C 273 (360 h_{70}^{-1} kpc from RX J1230.8+0115) at the redshift of the strong H I absorber ($cz_{\rm abs} = 1589$ km s^{-1}) analyzed by T2002. This galaxy has the spectroscopic signatures of a "poststarburst," a rare galaxy type in the local universe. The starburst phase might be expected to create a substantial wind that could be responsible for a high column

[2] The WIYN Observatory is a joint facility of the University of Wisconsin, Indiana University, Yale University, and the National Optical Astronomy Observatory.

density, low-ionization absorber like the one present in the 3C 273 sight line (J. T. Stocke et al. 2003, in preparation). While this galaxy is too far from RX J1230.8+0115 to be related to the $z = 0.005668$ complex, the fact that this object was missed by Morris et al. (1993) because of a classification error suggests that the region around RX J1230.8+0115 may not have been surveyed well enough to declare that similar luminosity galaxies have not been missed. No other galaxies were found in these observations at Virgo distances.

3. The WIYN/HYDRA observations concentrated on the region between RX J1230.8+0115 and 3C 273, 0.°9 to the north. The fiber setup for these observations was centered at R.A. $= 12^{h}30^{m}00^{s}$ and decl. $= +01°40'00''$ (J2000.0) and redshifts were obtained for 81% of the galaxies within a 20′ radius of this position. A total of 38 galaxies were observed successfully; only one galaxy was observed at both WIYN and LCO, as we worked to prevent duplication as much as possible. Thus, in the region north of RX J1230.8+0115, toward 3C 273, our galaxy survey is ~80% complete down to $m_B \leq 18.7$. No galaxies were found at Virgo distances in the WIYN/HYDRA observations either.

The galaxy survey work should provide some confidence that this region of space has been scrutinized exceptionally well for galaxies. There are 17 galaxies with $cz \leq 2500$ km s^{-1} now known in the region within 1 Mpc of either sight line. The SDSS (Stoughton et al. 2002) and the Morris et al. (1993) galaxy survey work is almost completely overlapping in the RX J1230.8+0115 region to an absolute magnitude limit of $M_B \simeq -14$. The CfA and J. T. Stocke et al. (2003, in preparation) survey work suggests that all relatively bright galaxies ($M_B \leq -16$) have been identified in the field and that only extremely faint ($M_B \leq -12$), extremely compact, or extremely low surface brightness galaxies could have been missed within 36 h_{70}^{-1} kpc of the sight line. A summary of the nearest galaxy to each of the absorbers is included in Table 3, which lists by column (1) target sight line, (2) Lyα absorber redshift (we list only the centroid of the absorption blend modeled here), (3) the heliocentric absorber velocity in km s^{-1}, (4) the velocity difference in the sense of ($V_{abs} - V_{gal}$) in km s^{-1}, (5) the impact parameter in h_{70}^{-1} Mpc, and (6) the name of the nearest galaxy to each absorber. The relationship between the Lyα absorbers and seven of these galaxies has been discussed extensively by Penton et al. (2002). The galaxy Leda 139866 is at 2329 km s^{-1}, just out of the velocity range discussed by Penton et al. (2002), and the "new galaxy" is the poststarburst galaxy described briefly above. The galaxy labeled [ISI96] 1228+0116 is a very low surface brightness dwarf irregular ($M_B \approx -13.6$; Impey et al. 1996).

Ten of the 17 galaxies near RX J1230.8+0115 and 3C 273 have recession velocities within ±300 km s^{-1} of the $z = 0.005668$ complex, but all are at substantial impact parameters (280–520 h_{70}^{-1} kpc). The nearest galaxy is an edge-on spiral of modest luminosity (CGCG 014−064; $M_B = -16.2$) located 279 h_{70}^{-1} kpc away with a redshift nearly identical to that of one of the absorbers in this complex. If the galaxies responsible for absorption at large impact parameters are expected to be bright, there is a much brighter, face-on spiral (NGC 4517A; $M_B = -18.8$) a little farther away, $\rho = 365$ h_{70}^{-1} kpc, with a larger velocity difference ($cz_{gal} = 1530$ km s^{-1}). On the other hand, it has been argued that low surface brightness (LSB) galaxies may be responsible for much of the Lyα absorption that we see. There is an LSB galaxy, discovered by Impey, Bothun, & Malin (1988), in the field, but it is even farther away in impact parameter (423 h_{70}^{-1} kpc) and velocity ($cz = 1473$ km s^{-1}). However, the velocity is similar to that of the absorber at $cz = 1482$ km s^{-1} (see Table 1). Identification of this LSB galaxy with the 1482 km s^{-1} absorber is problematic since there are three other galaxies within ±350 km s^{-1} that are similar distance or closer to RX J1230.8+0115 on the sky.

5. ABSORBER SIZES AS INFERRED FROM LINE-PAIR STATISTICS

The only "direct" measurement of the physical sizes of Lyα absorbers comes from the statistical analysis of line pairs in adjacent sight lines (see e.g., Foltz et al. 1984; Dinshaw et al. 1997). In summarizing recent results, Dinshaw et al. (1998) showed that the statistics of line pairs suggest characteristic *radii* for high column density ($\log N_{H\,I} \geq 14.5$ cm^{-2}; i.e., higher column density than the bulk of the Lyα forest) absorbers of 300–700 h_{70}^{-1} kpc for spherical clouds, with a possible trend toward larger sizes at smaller redshifts. The lowest redshift previously investigated using this technique is one pair of sight lines at $z \sim 0.5$ (Dinshaw et al. 1997). The maximum likelihood analysis used on these pairs provides a range of radii extending more than a factor of 2 on either side of the values quoted above. However, all of the radius estimates are comparable to, or larger than, typical distances between bright galaxies. Thus, if these absorber radii are interpreted as being "contiguous" structures, it is unlikely that Lyα absorbers are physically or causally

TABLE 3

DISTANCES FROM GALAXIES IN THE RX J1230.8+0115 AND 3C 273 FIELDS

Absorption System (1)	z_{abs} (2)	V_{abs} (km s^{-1}) (3)	ΔV (km s^{-1}) (4)	D_{perp} (Mpc) (5)	Nearest Galaxy (6)
RX J1230.8+0115-1	0.002963	888	−218	0.117	CGCG 014−054
RX J1230.8+0115-2	0.003437	1030	−76	0.117	CGCG 014−054
RX J1230.8+0115-3	0.004945	1482	184	0.271	HI 1225+01
RX J1230.8+0115-4	0.005668	1699	56	0.279	CGCG 014−064
RX J1230.8+0115-5	0.006148	1843	200	0.279	CGCG 014−064
RX J1230.8+0115-6	0.007680	2302	13	0.162	[ISI96] 1228+0116
3C 273-1	0.00337	1010	−96	0.104	CGCG 014−054
3C 273-2	0.00530	1589	33	0.071	New galaxy
3C 273-3	0.00745	2233	−96	0.396	Leda 139866

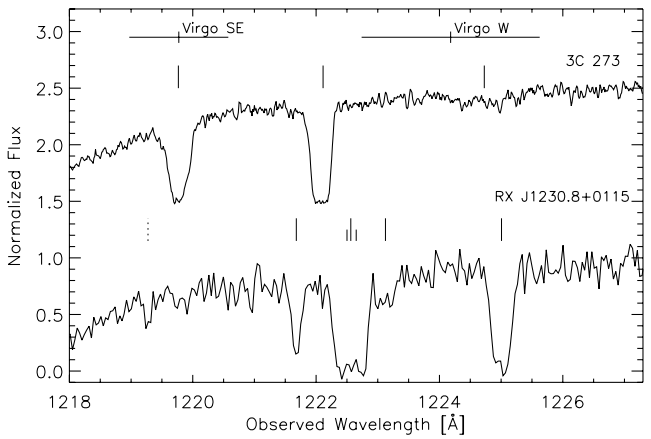

FIG. 7.—3C 273 (*top*) and RX J1230.8+0115 (*bottom*) spectra in the Virgo region. The ticks indicate the position of the absorbers (*solid line:* greater than 4 σ; *dotted line:* greater than 3.5 σ) in each sight line. The smaller ticks indicate the positions of the metal lines in the RX J1230.8+0115 spectrum. The crosses at the top of the figure indicate the velocity ranges for the Virgo galaxy "clouds," which encompass most of the velocity space covered by the absorbers. There is also general correspondence in velocity between most of the absorption systems in the two lines of sight, yet the profiles and depths of the lines are extremely different.

related to individual galaxies since their sizes are comparable to or larger than the distances between bright galaxies. These radii are more consistent with large-scale structure filaments found in numerical simulations (Davé et al. 1999). Additionally, the observation that not all absorbers found in one sight line have corresponding absorption in the other sight line implies that these are elongated structures rather than enormous spherical halos if the structures are "contiguous." An alternative explanation is that coincident line pairs indicate "correlated" structures of smaller systems, as in the case of galaxy halos aligned along a large-scale structure filament (see discussion in Dinshaw et al. 1994, 1997). This is suggested in several cases where substantial velocity and EW differences between coincident lines are noted (Dinshaw et al. 1994).

The pairs analysis of these sight lines is consistent with the inferences obtained from other sight-line pairs (Bechtold 1994; Crotts et al. 1994; Dinshaw et al. 1997, 1998). Figure 7 shows the 3C 273 (*top*) and RX J1230.8+0115 (*bottom*) spectra with the locations all greater than 4 σ (*solid ticks*) and greater than 3.5 σ (*dotted ticks*) absorbers marked as well as the velocity range for the two Virgo Supercluster "clouds" of galaxies in this direction. We note that the line pairs we have identified include absorbers with equivalent widths a factor of 4 less than those identified in the higher redshift studies of Dinshaw et al. (1997, 1998). Using the $\Delta v \leq 150$ km s^{-1} criteria for "coincident" line pairs suggested by Dinshaw et al. (1997), two of the three 3C 273 absorbers are coincident with 4 σ absorbers in the other sight line and the third is coincident with a marginal detection. For RX J1230.8+0115, four of five are coincident by the Dinshaw et al. (1997) definition by counting the 1685 and 1721 km s^{-1} absorbers as a single blended line and noting that the 1482 km s^{-1} absorber is also coincident with the same absorber in the 3C 273 sight line (thus, three "coincidences" if this sort of double counting is not justified). In either case, a large fraction of coincidences are present, suggesting that transverse sizes are large for at least some of these absorbers. The transverse distances between the sight lines at these redshifts is 200–500 h_{70}^{-1} kpc, assuming a pure Hubble flow in this direction, comparable to those investigated using other sight line pairs. The lowest velocity absorbers beyond Virgo (and thus at higher redshifts than shown in Fig. 7) have no coincident absorbers in the other sight line (Penton et al. 2000a) for transverse distances in the range 1.75–2.0 h_{70}^{-1} Mpc. These coincidences indicate characteristic Lyα absorber *radii* of $\sim$100–250 h_{70}^{-1} kpc. Unlike at higher redshifts, no chance pairings are expected in this velocity interval, which could confuse these issues. Using the line densities found by Penton et al. (2000b) at low H I column densities, we compute that there should be 0.14 ± 0.08 (a Poisson probability of 4×10^{-4}) line pairs with $\Delta v \leq 150$ km s^{-1} created by chance in Figure 7. Thus, all the absorber matches seen in these two spectra are real (to 99.96% confidence) statistical associations of absorbers.

The only coincidence between the H I and O VI absorber at 1011 km s^{-1} in the 3C 273 sight line and RX J1230.8+0115 is with the marginal detection at 889 km s^{-1}. While this is only a single incidence, a size limit of $\leq 225\ h^{-1}$ kpc (the distance between these two sight lines at this redshift) supports the collisionally ionized model for this absorber advocated by T2002, because a photoionized model for this absorber requires a very large physical size; i.e., we would expect a very large photoionized absorber to be more uniform over these two sight lines. As shown by examples in Tripp et al. (2001) and Tripp & Savage (2000), the simultaneous presence of O VI and absence of C IV absorption may be a discriminator between collisionally ionized and photoionized O VI absorbers.

The characteristic radii derived above are based on using the $\Delta v \leq 150$ km s^{-1} criterion, which was defined as a "coincidence" for much poorer resolution FOS spectra ($\approx$25 times poorer than the present data). If these spectra were smoothed to the FOS resolution (T. M. Tripp 2003, private communication), only one line-pair match and two mismatches would be found—the lower equivalent width lines in Figure 7 would not be detectable. The remaining coincidence includes the three metal-line absorbers at 1586–1721 km s^{-1}, suggesting a somewhat smaller but still substantial characteristic size for these structures. While the difference in these results is indicative of the resolution and sensitivity-dependent nature of this measurement, we would still conclude that these structures are large and elongated, comparable in size to the distance between these two sight lines.

Assuming that these absorbers reside in a gaseous filament with little turbulent motion, the Hubble flow velocity differences between absorbers in the two sight lines should be in the range 30–60 km s^{-1}. Therefore, despite the better STIS resolution and sensitivity, the $\Delta v \leq 150$ km s^{-1} criterion for absorber coincidences still seems reasonable over such large separations. While line-pair matches within 150 km s^{-1} suggest a relationship between these absorber pairs, the velocities, equivalent widths, and profile shapes are not so well correlated as to require "contiguous" structures stretching across these two sight lines (see, e.g., Rauch et al. 2001 examination of subkiloparsec separated sight lines at high z). However, we cannot rule out the existence of a low column density ($\log N_{\rm H\,I} \sim 13$ cm^{-2}) contiguous structure, augmented at specific locations by higher column density gas; e.g., galaxy halos or winds embedded in a large-scale gaseous filament. The presence of a galaxy at similar veloc-

ity to the 1586 km s^{-1} absorber and at a small impact parameter from 3C 273 (T2002 and Penton et al. 2002) may be evidence for this interpretation.

The small number of absorbers found in these two sight lines and the possible "special conditions" of the Virgo Cluster make statistical inference based upon this one sight-line pair insecure. However, the approximate velocity coincidence between the metal-line systems studied in detail here and in T2002 strongly suggests that these absorbers are related. We discuss the sizes and shapes of the absorbers implied by these pairing further in the discussion section.

6. DISCUSSION AND CONCLUSIONS

The absorption-line systems in the RX J1230.8+0115 and 3C 273 sight lines along the southern edge of the Virgo Cluster provide a low-redshift laboratory in which to study the properties of these absorbers and their relationship with their environment. We have presented a detailed discussion of the physical properties of these absorbers, concentrating on the characteristic sizes of low-z Lyα absorbers. We summarize these results in the next subsection. In § 6.2 we present an interpretation of the nature of these absorbers inferred from their properties and from the local environment of the Lyα absorption systems and present our conclusions about these absorbers.

6.1. *Properties of the Absorbers*

Based upon a detailed photoionization equilibrium calculation, the two blended absorbers in the RX J1230.8+0115 sight line at 1685 and 1721 km s^{-1} and the 1586 km s^{-1} absorber in the 3C 273 sight line (T2002) have inferred sizes along the line of sight of $\sim$20 kpc and 70 pc, respectively. These inferences are much more secure for the 3C 273 absorber because the hydrogen column density can be accurately determined because of available high-quality *FUSE* spectroscopy of the higher order Lyman lines. For the 3C 273 absorber, T2002 find $\log N_{\rm H\,I} = 15.85$ cm^{-2}, $\log(n_{\rm H}) = -2.8 \pm 0.3$ cm^{-3}, $Z = 0.06\,Z_{\odot}$, and an inferred thickness of $\sim$70 pc. For the case of the two blended absorbers studied here, the combination of *HST* STIS echelle and *FUSE* spectroscopy are insufficient to provide similarly tight constraints. The *FUSE* spectrum is sufficient to rule out column densities as low as 10^{15} cm^{-2} and set a probable lower limit of $N_{\rm H\,I} = 10^{16}$ cm^{-2} for each absorber due to significant detections of Lyγ and Lyδ in both components and possible detections of Lyϵ, Lyη, and Lyθ in at least one component. Additionally, the low b-values that would be required to fit Lyα rule out column densities above $\log N_{\rm H\,I} = 17.0$ cm^{-2}.

We use the available STIS echelle and *FUSE* data to infer the physical conditions of these absorbers. The metal-line ratios [N(C IV)/N(C II) and N(Si IV)/N(Si II)] constrain the ionization parameter ($-2.85 < \log U < -2.60$) for our best-guess model, assuming the gas is photoionized. Assuming a standard value for the extragalactic ionizing radiation intensity, we can translate this to limits on the density of the gas. If we knew the metallicity of these structures, this would constrain the hydrogen column density and thus the absorber size along our line of sight. By assuming the same metallicity for these absorbers as for the 3C 273 absorber located some 350 h_{70}^{-1} kpc away and column densities of $\log N_{\rm H\,I} = 16$–17, consistent with constraints from the STIS and *FUSE* data, we calculate line-of-sight sizes of 10–30 kpc. Since these metallicities and column densities are similar to those obtained by T2002, the larger physical sizes obtained here are due to the higher ionization (lower density) of the RX J1230.8+0115 absorbers (C IV is detected here, but not in 3C 273). The blended absorbers studied here have inferred line-of-sight sizes a factor of 7–300 times less than the minimum transverse size based upon detecting absorption in both sight lines at comparable redshifts, while the 1586 km s^{-1} absorber in 3C 273 has a size that is a factor of $\sim$4300 smaller than the minimum transverse size. This much larger inferred transverse size is more suggestive of objects associated with large-scale structure than with individual galaxies, while the smaller line-of-sight sizes are more consistent with structures related to individual galaxies (e.g., very extended halos or outflowing winds).

While only a few high column density absorbers similar to the ones in these two sight lines are known, they are not unique at low redshift. There is an absorber with a column density of $\log N_{\rm H\,I} \sim 16$ cm^{-2} at $z = 0.167$ toward PKS 0405-1219 (Chen & Prochaska 2000) and one with a column density of $\log N_{\rm H\,I} = 15.57$ at $z = 0.22497$ toward H1821+643 (Tripp, Savage, & Jenkins 2000; Oegerle et el. 2000). Both of these systems very closely resemble the RX J1230.8+0115 $z = 0.005668$ complex in that they all contain a saturated absorber with a two-component metal-line system. These absorbers also have nearby galaxies, there is an $0.02L_K^*$ spiral galaxy at 90 h_{70}^{-1} kpc and a $1.2L_K^*$ elliptical at 110 h_{70}^{-1} kpc from PKS 0405−1219 and there is a galaxy 112 h_{70}^{-1} kpc away from the H1821+643 absorber. The difference between the RX J1230.8+0115 $z = 0.005668$ complex and these systems is the existence of higher ionization species detected with O VI and N V detected in PKS 0405−1219 and O VI and Si III detected in H1821+643.

At somewhat higher redshifts, Rigby et al. (2002) identify a class of weak Mg II systems that have similar physical properties to the absorbers discussed above including sizes on the order of 10 pc to several kiloparsecs. For the limited number of regions around the absorbers that have been surveyed optically, there are no galaxies down to $0.01L^*$ within 70 h_{70}^{-1} kpc, but larger regions around the absorbers have not been studied.

While the lower ionization weak Mg II absorbers are most similar to the absorbers studied here and in the 3C 273 sight line, there are also more highly ionized metal-line absorbers (i.e., O VI detected) that are found somewhat farther from galaxies but that seem to be associated with galaxy groups. The PKS 2155−304 sight line has six absorbers between 16,000 and 18,000 km s^{-1}, which appear to be associated with a small group of spiral galaxies, although none of these are within 400 h_{70}^{-1} kpc of the absorbers (Shull et al. 1998). Two of these absorbers have been detected in O VI with *FUSE* (J. M. Shull et al. 2003, in preparation), and there is a tentative detection of O VIII with *Chandra* (Fang et al. 2002). The two O VI absorbers in the PG 0953+415 sight line (Savage et al. 2002) fall near peaks in the galaxy density, with the $z = 0.14232$ absorber having four galaxies within 130 km s^{-1} and 3 Mpc, the closest at a projected distance of 395 kpc (Tripp & Savage 2000). Similarly, the H1821+643 $z = 0.1212$ absorber appears to fall within a galaxy group, with seven galaxies within 500 km s^{-1} and 3.1 Mpc. These higher ionization absorbers have larger inferred line-of-sight sizes than those discussed above (based on a photoionization model). However, since there are no adjacent sight lines, there are no constraints on their transverse sizes.

We note that the column densities of the absorbers studied here are unusually high for the bulk of the local Lyα forest absorbers and so are probably not representative of the properties (size, metallicity, etc.) or the environment of the lower column density lines ($\log N_{\rm H\,I} < 14$ cm^{-2}; Penton et al. 2002).

6.2. *Galaxy/Absorber Associations and Large-Scale Structure*

Penton et al. (2002) examined the hypothesis that the 3C 273 and RX J1230.8+0115 absorbers at Virgo distance are due to extended galaxy halos and concluded that the evidence was inconsistent with the available data. Based upon the known galaxy redshifts, the nearest galaxies to the strong absorbers in these sight lines were $\geq 200\ h_{70}^{-1}$ kpc away, and there seemed to be no correlation between impact parameter and the probability of detecting absorption as would be expected in a simple halo model. The galaxy redshift surveys have been improved, and a dwarf galaxy has been found only 71 h_{70}^{-1} kpc from the 3C 273 1586 km s^{-1} absorber (J. T. Stocke et al. 2003, in preparation). Finding this galaxy may indicate that the halos of dwarf galaxies or outflows from them are responsible for some Lyα absorbers. The "poststarburst" signature in the optical spectrum of this galaxy makes an outflow model for the 3C 273 absorber particularly attractive since it can explain the subsolar metal abundances as well as the supersolar (Si/C) ratio, which is indicative of SN type II enrichment.

The RX J1230.8+0115 $z = 0.005668$ complex could be associated with a gas-rich galaxy (H I 1225+01) 400 km s^{-1} and 270 h_{70}^{-1} kpc away, or with the edge-on dwarf spiral (CGCG 014−064) 280 h_{70}^{-1} kpc and only 56 km s^{-1} away. The fact that the dwarf galaxy 71 h_{70}^{-1} kpc from 3C 273 was missed by Morris et al. (1993) provides a warning that the RX J1230.8+0115 region may not have been surveyed sufficiently well to conclude that there are no galaxies of similar luminosity near these blended absorbers, although there have been a number of relatively deep, independent surveys of this region. If another faint galaxy is found close to RX J1230.8+0115 at $cz \sim 1700$ km s^{-1}, then the model of outflowing winds from dwarf galaxies (J. T. Stocke et al. 2003, in preparation) is an exceptional fit for both the 3C 273 and RX J1230.8+0115 $cz \sim 1700$ km s^{-1} absorbers (J. T. Stocke et al. 2003, in preparation). The higher than average galaxy density ($\approx$50 times the average) in this region at the southern edge of the Virgo Cluster make this a reasonable possibility. However, this scenario may require very large amounts of H I associated with quite small galaxies (see below and J. T. Stocke et al. 2003, in preparation for further discussion).

RX J1230.8+0115 is 0.°9 from 3C 273, and both of these lines of sight pass through a filament of galaxies identified by Penton et al. (2002) as well as passing through the Virgo Southern Extension and near the W cloud (the W′ cloud, discussed as part of this region by T2002, lies several degrees to the north; Binggeli, Popescu, & Tammann 1993). These galaxy clouds are thought to be independent of the Virgo Cluster. The W cloud is a large feature that may be another filament stretching to the north at higher velocities than are found in the Penton et al. (2002) filament. However, the SE cloud is embedded in the northern end of this filament. Penton et al. (2002) showed that both of the strong 3C 273 Virgo absorbers, all of the RX J1230.8+0115 Virgo absorbers, plus the seven (now eight) known galaxies in the region all lie along a single large-scale structure filament that could extend for many Mpc crossing these sight lines.

The filamentary model for these absorbers is consistent with the abundance of common velocity ($\pm$150 km s^{-1}) absorber pairs seen in these two sight lines but *not* with the line-of-sight thicknesses of these structures inferred from photoionization models. Either the methods used to estimate absorber sizes could be wrong—a very thin "ribbon" or "sheet" of gas could extend along this filament of galaxies for at least several hundred kiloparsecs—or, because the pairs analysis cannot distinguish between "contiguous" or "correlated" structures as emphasized by its practitioners (Dinshaw et al. 1997), these absorbers map out correlated rather than contiguous structures. Given the difference in depth versus transverse size for these absorbers and the lack of detailed correlations between the absorber properties (i.e., velocity differences greater than $\pm$50 km s^{-1}, which could be accounted for by Hubble flow, as well as large equivalent width differences; see § 5) in these two sight lines, a correlated structure model seems much more plausible. One possibility is that the absorbers in this correlated structure are related to individual galaxies whose halos or outflowing winds have caused significant clumping and metal enrichment in small regions of the large gaseous structure in which they are embedded. If this is the case, we might expect to find one or more faint galaxies close to the RX J1230.8+0115 Virgo absorbers.

The high-resolution STIS echelle spectra, shown in Figure 7, indicate that there is no detailed correlation between the velocities or the equivalent widths of the absorbers in these sight lines. These differences in velocity and equivalent width structure contrast with the extremely detailed velocity and equivalent width correlations between the Lyα absorbers in the two gravitationally lensed images of Q1422+231 (Rauch et al. 2001) separated by 80 h_{70}^{-1} pc at $z = 3.3$. In the case of the Q1422+231 absorbers there is a detailed agreement between these absorber properties, requiring a quiescent, contiguous gaseous structure (Rauch et al. 2001). The differences between the Q1422+231 sight lines and these sight lines may indicate the difference in scale over which we see contiguous structures (tens of parsecs) and correlated structures (hundreds of kiloparsecs).

If we assume that the absorber depths of 1–30 kpc calculated in § 3 and in T2002 are indicative of the overall three-dimensional size of these absorbers, then, in order to obtain a covering factor of unity (as would be required to detect three such absorbers in the two sight lines observed), there would need to be 10–10,000 of these structures in the filament (assuming a filament thickness of $\sim$100 kpc). Charlton et al. (2002) also find that a large number of weak Mg II absorbing structures are required to explain their detected population found at higher redshifts; i.e., these absorbers must greatly outnumber bright galaxies. Although not yet observed at Mg II, the three absorbers discussed here are very similar to those studied by Charlton et al. (2002). If these absorbers are associated with galaxies, we would expect to find numerous faint or low surface brightness galaxies throughout this filament. While we make the case in § 6 that some galaxies may have been missed, this filament has been thoroughly surveyed for galaxies and only eight have been found. It is very hard to believe that large numbers of star formation sites have been missed given the volume of galaxy redshift data available for this region (§ 4).

One possible scenario is that while these absorbers have small thicknesses, they could be quite extended on the sky if the metal enriched gas is in the form of a thin shell surrounding a galaxy, perhaps driven by a wind. In this case, the area on the sky would be substantially larger than the thickness derived from photoionization; e.g., the radius of the shell could extend 50–100 h^{-1} kpc from the galaxy if the distance to the galaxy near the 3C 273 absorber is indicative of the size of these shells (impact parameter = 71 h^{-1} kpc; § 4 and J. T. Stocke et al. 2003, in preparation). In this case, only a few ($\sim$4) gaseous shells would be required to have the covering fraction of unity necessitated by the 3C 273/RX J1230.8+0115 observations. In the shell scenario, it would also be quite natural to find two absorbers closely spaced in velocity along a single sight line (e.g., RX J1230.8+0115) as a result of intercepting both sides of the expanding shell of gas. For a 75 kpc radius shell with an expansion velocity of 18 km s^{-1} (half the separation between the RX J1230.8+0115 metal lines) the epoch of star formation would have occurred $\sim 4 \times 10^9$ yr ago expelling 7×10^9 $M_\odot$ of gas (given the average RX J1230.8+0115 gas density and shell thickness). Thus, the galaxy putatively associated with the enriched gas in these absorbers does not need to be currently forming stars. This is the case for the dwarf near the 3C 273 absorber (J. T. Stocke et al. 2003, in preparation), which would have had to expel $\sim 2 \times 10^8$ $M_\odot$ of gas in this scenario. This scenario requires large masses of gas to have been expelled from galaxies but may be compelling if another galaxy is found near RX J1230.8+0115. Given the significant amount of optical spectroscopy already expended on this region, it may be more likely that the column density of the absorber is on the high end of our range, making the metallicity significantly smaller. In this lower metallicity scenario, these systems could represent more primordial overdensities expected to be associated with large-scale structure (Davé et al. 1999; Stocke et al. 2001; Penton et al. 2002). Given the proximity of these absorbers to us, this region is the best available laboratory with which to test this hypothesis, so we are presently surveying the region at the 21 cm line of H I to look for gas-rich galaxies as well as continuing our optical spectroscopy to answer this question definitively.

J. L. R. thanks Steve Penton for assistance extracting and calibrating the RX J1230.8+0115 STIS spectrum and Ken Sembach for input on the *FUSE* spectrum. The authors thank Todd Tripp for an extremely careful reading of the paper and helpful suggestions. J. T. S., M. L. G., and J. L. R. acknowledge financial support from NASA-*HST* Archival Research Grant AR-09221.01-A and Guest Observer grant GO-08182.01 for this work. J. T. S. also acknowledges support for the Cosmic Origins Spectrograph GTO Team through NAG 512279. J. T. S. thanks Ray Weymann and Kevin McLin for permission to quote some results from our galaxy survey work in the RX J1230.8+0115 and 3C 273 region prior to publication.

REFERENCES

Bahcall, J., et al. 1991, ApJ, 377, L5
Bechtold, J. 1994, ApJS, 91, 1
Bechtold, J., Crotts, A. P. S., Duncan, R. C., & Fang, Y. 1994, ApJ, 437, L83
Binggeli, B., Popescu, C. C., & Tammann, G. A. 1993, A&AS, 98, 275
Bowen, D. V., Pettini, M., & Blades, J. C. 2002, 2002, ApJ, 580, 169
Charlton, J. C., Churchill, C. W., Ding, J., Zonak, S., Bond, N., & Rigby, J. R. 2002, in ASP Conf. Ser. 254, Extragalactic Gas at Low Redshift, ed. J. Mulchaey & J. Stocke (San Francisco: ASP), 254, 122
Chen, H.-W., & Prochaska, J. X. 2000, ApJ, 543, l9
Crotts, A. P. S., Bechtold, J., Fang, Y., & Duncan, R. C. 1994, ApJ, 437, L79
Davé, R., Hernquist, L., Katz, N., & Weinberg, D. H. 1999, ApJ, 511, 521
Davé, R., & Tripp, T. M. 2001, ApJ, 553, 528
Dinshaw, N. D., Foltz, C. B., Impey, C. D., & Weymann, R. J. 1998, ApJ, 494, 567
Dinshaw, N. D., Weymann, R. J., Impey, C. D., Foltz, C. B., Morris, S. L., & Ake, T. 1994, ApJ, 437, L87
———. 1997, ApJ, 491, 45
Donahue, M. E., Aldering, G., & Stocke, J. T. 1995, ApJ, 450, L45
Fang, T., Marshall, H. L., Lee, J. C., Davis, D. S., & Canizares, C. R. 2002, ApJ, 572, L127
Ferland, G. J. 1996, HAZY, a Brief Introduction to Cloudy (Univ. Kentucky Dept. Phys. Astron. Int. Rep.)
Foltz, C. B., Weymann, R. J., Roser, H.-J., & Chaffee, F. H. 1984, ApJ, 281, L1
Grogin, N. A., Geller, M. J., & Huchra, J. P. 1999, ApJS, 119, 277
Haardt, F., & Madau, P. 1996, ApJ, 461, 20
Heap, S. R., Williger, G. M., Davé, R., Weymann, R. J., Jenkins, E. B., & Tripp, T. M. 2002, in ASP Conf. Ser. 254, Extragalactic Gas at Low Redshift, ed. J. Mulchaey & J. Stocke (San Francisco: ASP), 63
Hwang, U., Mushotzky, R. F., Loewenstein, M., Markert, T. H., Fukazawa, Y., & Matsumoto, H. 1997, ApJ, 476, 560
Impey, C., & Bothun, G. 1997, ARA&A, 35, 267
Impey, C., Bothun, G., & Malin, D. 1988, ApJ, 330, 634
Impey, C., Sprayberry, D., Irwin, M. J., & Bothun, G. 1996, ApJS, 105, 209
Lanzetta, K. M., Bowen, D. V., Tytler, D., & Webb, J. K. 1995, ApJ, 442, 538
Lin, W. P., Börner, G., & Mo, H. J. 2000, MNRAS, 319, 517
Maloney, P. 1993, ApJ, 414, 41
McLin, K., Stocke, J. T., Weymann, R. J., Penton, S. V., & Shull, J. M. 2002, ApJ, 574, L115
Morris, S. L., & van den Bergh, S. 1994, ApJ, 427, 696
Morris, S. L., Weymann, R. J., Dressler, A., & McCarthy, P. J. 1993, ApJ, 419, 524
Morris, S. L., Weymann, R. J., Savage, B. D., & Gilliland, R.L. 1991, ApJ, 377, L21
Oegerle, W. R., et al. 2000, ApJ, 538, L23
Penton, S. V., Shull, J. M., & Stocke, J. T. 2000a, ApJ, 544, 150
———. 2002, ApJ, 565, 720
Penton, S. V., Stocke, J. T., & Shull, J. M. 2000b, ApJS, 130, 121
———. 2003, ApJ, submitted
Rauch, M., Sargent, W. L. W., Barlow, T. A., & Carswell, R. F. 2001, ApJ, 562, 76
Rigby, J. R., Charlton, J. C., & Churchill, C. W. 2002, ApJ, 565, 743
Savage, B. D., & Sembach, K. R. 1991, ApJ, 379, 245
Savage, B. D., Sembach, K. R., Tripp, T. M., & Richter, P. 2002, ApJ, 564, 631
Schaye, J. 2001, ApJ, 559, 507
Sembach, K. R., Howk, J. C., Savage, B. D., Shull, J. M., & Oegerle, W. R. 2001, ApJ, 561, 573
Shull, J. M., Penton, S., Stocke, J. T., Giroux, M. L., van Gorkom, J. H., Lee, Y. H., & Carilli, C. 1998, AJ, 116, 2094
Shull, J. M., Roberts, D., Giroux, M. L., Penton, S. V., & Fardal, M. A. 1999, AJ, 118, 1450
Southerland, R. S., & Dopita, M. A. 1993, ApJS, 88, 253
Steidel, C. C. 1995, in QSO Absorption Lines, ed. G. Meylen (Garching: Springer), 139
Stocke, J. T., Shull, J. M., Penton, S. V., & Gibson, B. K. 2001, in ASP Conf. Ser. 240, Gas and Galaxy Evolution, ed. J. E. Hibbard, M. Rupen, & J. H. van Gorkom (San Francisco: ASP), 21
Stoughton, C., et al. 2002, AJ, 123, 485
Tonry, J. L., Blakeslee, J. P., Ajhar, E. A., & Dressler, A. 2000, ApJ, 530, 625
Tripp, T. M., Giroux, M. L., Stocke, J. T., Tumlinson, J., & Oegerle, W. R. 2001, ApJ, 563, 724
Tripp, T. M., & Savage, B. D. 2000, ApJ, 542, 42
Tripp, T. M., Savage, B. D., & Jenkins, E. B. 2000, ApJ, 534, L1
———. 2002, ApJ, 575, 697
Weymann, R. J., Rauch, M., Williams, R., Morris, S. L., & Heap, S.R. 1995, ApJ, 438, 650
Weymann, R. J., Vogel, S. N., Veilleux, S., & Epps, H. W. 2001, ApJ, 561, 559